JOURNAL OF AGRICULTURAL AND FOOD CHEMISTRY

J. Agric. Food Chem. **2006,** *54,* 517−522 **517**

Zein Dynamic Adsorption to Carboxylic and Alkyl Coated Surfaces

QIN WANG,[†] QIAN WANG,[‡] XUEJUN WANG,[‡] AND GRACIELA W. PADUA*,[†]

Department of Food Science and Human Nutrition, University of Illinois, 382/D AESB, 1304 West Pennsylvania Avenue, Urbana, Illinois 61801, and Department of Chemistry, University of Illinois, 51 RAL, 600 South Mathews Avenue, Urbana, Illinois 61801

The adsorption of a commercial zein sample on carboxylic (COOH) and alkyl (CH_3) surfaces was monitored by high time resolution surface plasmon resonance. Zein showed higher affinity and higher mass adsorption on carboxylic than alkyl surfaces. A zein layer specific for each surface was obtained after flushing off loosely bound zein with 75% 2-propanol solutions. Zein deposits were examined under atomic force microscopy. Differences in layer thickness between carboxylic and alkyl surfaces were explained in terms of zein adsorption footprint.

KEYWORDS: Zein; surface polarity; surface plasmon resonance; atomic force microscopy

INTRODUCTION

Zein is the alcohol-soluble fraction of corn proteins. It is markedly hydrophobic when compared to other proteins and has a remarkable ability to form films on hard surfaces. Zein has been studied for its potential as a novel biobased polymeric material. Free-standing zein films were prepared by incorporating oleic acid during film processing to increase film ductility (*1*). Quality differences observed in finished films were related to film structure, which in turn was believed to be affected by zein−oleic acid interactions.

In previous research, preparation of zein films was attempted using the methyl ester of oleic acid as plasticizer (*2*). Such films were stiff and brittle, pointing out the differences between oleic acid and methyl oleate as zein plasticizers. The experiment suggested that the carboxylic group (COOH) in oleic acid was critical to zein plasticization. Therefore, Wang and co-workers (*3*, *4*) studied static and dynamic interactions between zein and self-assembled monolayers (SAMs) of methyl-ended and carboxyl-ended hydrocarbon chains using surface plasmon resonance (SPR). SPR is a technique of high sensitivity and has often been used as a biosensor to study biomolecular interactions such as protein adsorption on polymer surfaces, DNA hybridization, and lipid membrane−protein interactions (*5*−*7*). Wang and co-workers (*3*, *4*) found that zein interacted with both methyl-ended and carboxyl-ended surfaces, represented by 1-octanethiol and 11-mercaptoundecanoic acid monolayers, respectively; however, rate of adsorption and total mass adsorption were higher on carboxylic than on alkyl surfaces. They also observed using atomic force microscopy (AFM) that zein deposits developed different morphologies when adsorbed to either surface.

During extraction, zein becomes in contact and adsorbs carotenoid pigments from corn. Further extraction and purification steps remove such pigments presumably modifying the protein surface with respect to the original extract. In this work we examined the adsorption behavior of low carotenoid content (LCC) zein on carboxylic and alkyl surfaces generated by self-assembled monolayers of 11-mercaptoundecanoic acid and 1-octanethiol by SPR. The objective was to compare its adsorption behavior with that of high carotenoid content (HCC) zein, which had been reported by Wang and co-workers (*4*). The topography of zein deposits was observed by AFM.

EXPERIMENTAL PROCEDURES

Materials. LCC zein was from Showa Sangyo Co., Ltd, Japan. HCC zein was of regular grade, F4000, lot # F4000318C, from Freeman Industries, Inc. Tuckahoe, NY. The reported protein content for the F4000 Zein was around 90% (dry basis). 11-Mercaptoundecanoic acid (MUA), 1-octanethiol (1-OT), and chloroacetic acid were from Aldrich Co., Inc., Milwaukee, WI. Ethyl alcohol and isopropyl alcohol were from Midwest Grain Products, Pekin, IL. 2,5-Dihydroxyl benzoic acid was from DHB, Sigma Chemical Co., St. Louis, MO.

Color Measurement. *L*, *a*, and *b* values of HCC zein and LCC zein samples were measured by Hunter Colorimetry (LabScan XE, HunterLab, Reston, VA). Samples in Petri dishes were placed at the specimen port to obtain instrument readings.

Matrix-Assisted Laser Deporption−Ionization Mass Spectrometry (MALDI/MS) Experiments. MALDI spectra were collected for HCC zein and LCC zein. Measurements were performed on a Voyager-DE STR system (Applied Biosystems, Inc., Foster City, CA) operating in a positive ion linear mode. Ions formed by a pulsed UV laser (nitrogen laser, $\lambda = 337$ nm) were accelerated at 25 kV. The various samples of zein were dissolved in 55% (v/v) 2-propanol/water at 5 mg/mL with 5% formic acid to promote dissolution. The supernatant after centrifugation was diluted 10 times with 10 mg/mL 2, 5-dihydroxyl benzoic acid used as matrix material.

Protein Content Measurement. The protein content of HCC zein and LCC zein was measured with a LECO protein/nitrogen determi-

* To whom correspondence should be addressed. Phone: (217) 333-9336. Fax: (217) 333-9329. E-mail: gwpadua@uiuc.edu.
[†] Department of Food Science and Human Nutrition.
[‡] Department of Chemistry.

10.1021/jf051545l CCC: $33.50
Published on Web 12/15/2005

Table 1. Color Measurement of Two Commercial Samples of Zein

	L	a	b
HCC zein	76.3	6.3	31.2
LCC zein	90.8	–0.2	7.0

nation system (FP-528, LECO Corp., St. Joseph, MI) using 0.2 g of each sample. The instrument determines protein content based on the nitrogen percentage of a standard sample.

SPR Sample Preparation. Zein solutions of LCC zein (0.10, 0.30, 0.50, and 1.00% zein w/v) were prepared by stirring the proper amount of zein in aqueous 75% (v of alcohol/v of alcohol and water) 2-propanol. The pH of aqueous alcohol was previously adjusted to 3.55−3.85 with chloroacetic acid. SPR substrates were gold-coated SF10 glass slides, which have a refractive index of 1.721. Before metal evaporation, SF10 glass slides (Schott Glass Technologies, Duryea, PA) were thoroughly cleaned in a 4:1, sulfuric acid:30% hydrogen peroxide cleaning solution at room temperature for 1 h. The dried slides were then coated with a 10-Å chromium (Kurt J. Lesker, Clairton, PA) adhesion layer at 0.1 Å/s and a 470−480-Å gold (99.99% purity) overlayer at 1.0 Å/s by resistive evaporation under a pressure of 4×10^{-7} Torr. Chromium was applied to ensure good adhesion of the gold layer since gold coatings can be easily peeled from glass. Samples were stored in N_2 before use. For the preparation of carboxylic acid terminated and methyl terminated SAMs, 1 mM ethanolic solutions of 11-mercaptoundecanoic acid ($COOH(CH_2)_{10}SH$) or 1-octanethiol ($CH_3(CH_2)_7SH$) were pumped past gold coated slides in the SPR flow cell for 40 min.

SPR Measurement. The SPR measurements were conducted in a custom-built instrument. A 650-nm linearly polarized, single-mode diode laser with an output of approximately 4 mW was spatially filtered and adjusted to p polarization. A cylindrical lens focused the light into a line focus on an Au film, which was deposited on the base of a SF10 glass slide and mounted in the Kretschmann configuration. A Kel-F flow cell covers the active side of the Au film, with a volume of approximately 150 μL. A Masterflex variable-speed pump with a flow-rate range of 0−10 mL/min was used to control solution flow rate through the cell. The flow rate used in this experiment was 0.5−1.0 mL/min. The resonance was monitored in real time by imaging the angular dispersion of the light reflected from the Au film on a charge-coupled device camera (Photometrics PM512) using Photometrics CCD9000 software. The intensity profiles were fit to a polynomial from which the angle of minimum reflectance was extracted. Theoretical shifts associated with the adsorption of dielectric layers on the Au surface were calculated from intensity profiles created using a five-layer Fresnel system. Nonlinear least-squares fitting was performed by a Levenberg−Marquardt algorithm using IgorPro software (Wave-Metrics, OR). SPR results are given as averages of mass adsorbed per unit area.

AFM Experiment. AFM images were taken with a Nanoscope IIIa microscope (Dimension 3100, Digital Instruments Inc., Santa Barbara, CA) where the tip motion is followed by deflection of a laser beam reflected off the rear side of the cantilever. The deflection is monitored with a position-sensitive detector. All AFM images were taken with a rod-type scan head. Silicon tips (BudgetSensors, BS-Tap300AL with a resonance frequency of ~300 kHz and force constant around 40 N/m) attached to a microfabricated cantilever with a scan frequency of 1.5 Hz were used. Measurements were collected in the tapping mode, in which less force was applied to the scanned samples. In most experiments, images were taken repetitively changing the slide position. This procedure helps verify the observed structure and optimize the scan parameters and quality of recorded images. Samples of gold coated surfaces, SAMs, and zein deposits were examined by AFM.

RESULTS AND DISCUSSION

Color Comparison.

L, *a*, and *b* values for HCC zein and LCC zein samples are listed in **Table 1**. The Hunter *L* value characterizes the color of a sample by fixing its position on a light−dark axis. It varies from 100 for perfect white to 0 for black. The *L* value for LCC zein was around 90, which indicated a lighter color than that of HCC zein (76). The Hunter a value measures redness (+) to greenness (−). HCC zein showed more redness than the LCC zein sample. The Hunter *b* value measures yellowness (+) to blueness (−). HCC zein had a *b* value of 31, showing more yellow than LCC zein ($b = 7$). Zein yellowness was attributed to zeaxanthin and other carotenoids present in corn that attach themselves to the protein during extraction.

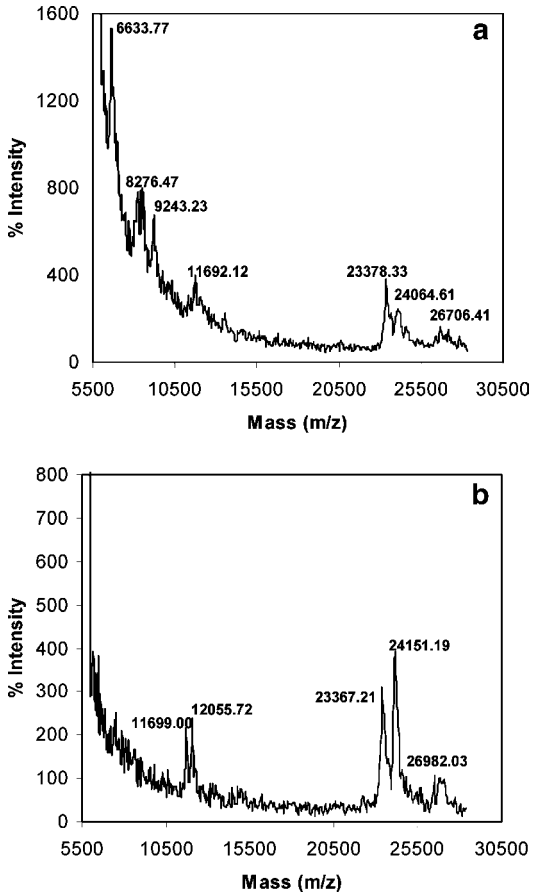

Figure 1. (**a**) Molecular weight distribution of HCC zein from MALDI. (**b**) Molecular weight distribution of LCC zein from MALDI.

MALDI/MS.

MALDI/MS was used to qualitatively characterize the molecular weight (MW) composition of the two commercial zein samples, which were extracted and purified using ostensibly different protocols. MW distribution of HCC and LCC zein is shown in parts a and b of **Figure 1**, respectively. Both zein samples had peaks around *m*/*z* 23 000−24 000 and 26 000, which are considered as α-zein under Esen (*8*) classification. Several peaks around *m*/*z* 12 000 appeared in both samples, which had also been observed by Wang et al. (*9*). MALDI peaks of *m*/*z* 12 000 were larger in LCC zein than HCC zein. This small MW peptide might also be contributed by α-zein, according to Esen's nomenclature.

Protein content of HCC zein was determined at 88.7%, while that of LCC zein was 98.2%. The difference was attributed to lipids, pigments, and residual starch. Dickey and co-workers (*10*) pointed out that zein is often associated with lipids. Although LCC zein had a higher protein content than HCC samples, both had similar protein MW profiles.

SPR Results.

Dynamic adsorption profiles of LCC zein from 75% 2-propanol solutions (0.1−1.0% w/w) on MUA SAMs and on 1-OT SAMs are shown in **Figures 2** and **3**, respectively. Adsorption

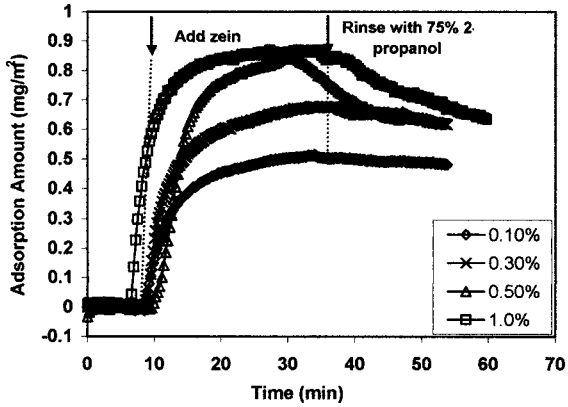

Figure 2. Zein adsorption kinetics from 75% 2-propanol slolutions onto SAMs of 11-mercaptoundecanoic acid for different zein bulk concentration levels.

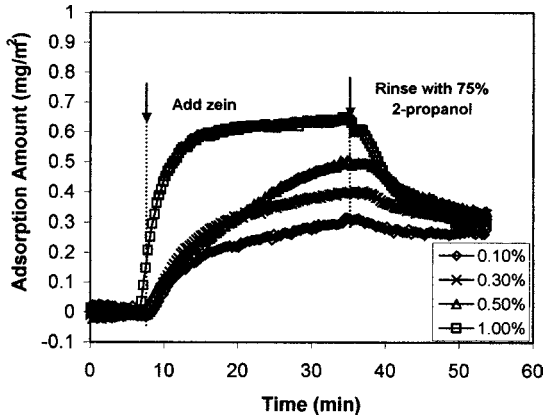

Figure 3. Zein adsorption kinetics from 75% 2-propanol slolutions onto SAMs of 1-octanethiol for different zein bulk concentration levels.

profiles have a similar shape for all concentrations on each of the two SAMs. At the start of the experiment, the amount of adsorbed protein increased linearly with time. When the surface became saturated, adsorption and desorption reached equilibrium and accumulation ceased. On each SAM, maximum adsorption increased with zein concentration, with the lowest at 0.31 mg/m^2 for alkyl surface at 0.1% and highest at 0.87 mg/m^2 for carboxylic surface at 1.0%. Maximum adsorption was higher on carboxylic than on alkyl surfaces.

The initial adsorption rate, $[d\Gamma/dt]_0$, or the slope of the linear portion of each adsorption profile, was plotted against concentration in **Figure 4**. For all concentration levels $[d\Gamma/dt]_0$ was higher on carboxylic than on alkyl surfaces. On 11-mercaptoundecanoic acid surfaces, $[d\Gamma/dt]_0$ was linear with zein concentration up to 0.5% ($R^2 = 0.91$), suggesting mass-transport-limited adsorption up to that concentration level. On 1-octanethiol surfaces, $[d\Gamma/dt]_0$ was considered linear through the concentration range ($R^2 = 0.97$). In this regression, the point corresponding to 0.5% zein was not included due to perceived anomalies in the behavior of that sample. At that concentration, zein was hard to adsorb on alkyl surfaces and easy to wash off from them. The average maximum adsorption was 0.25 mg/m^2 with a coefficient of variation of 0.67, which was high with respect to that of other solutions (i.e., 0.04 for 0.3% on carboxylic surface). Aggregation may have affected protein surface properties at this point. Zein adsorption on alkyl surfaces was thus considered mass-transport-limited throughout the concentration range. This conclusion is in agreement with Wang and co-workers (*4*) where HCC zein was observed to follow mass-transport-limited adsorption on alkyl surfaces. The same

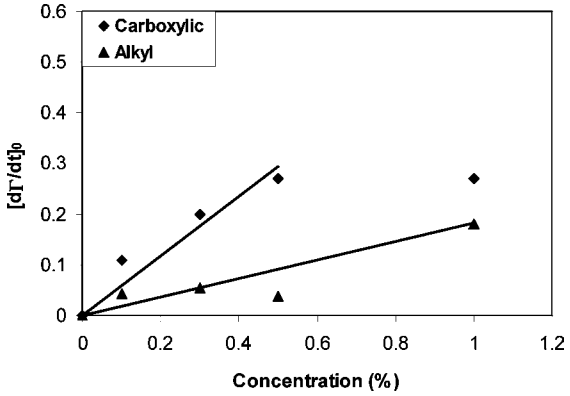

Figure 4. Initial rate of zein adsorption on carboxylic and on alkyl surfaces.

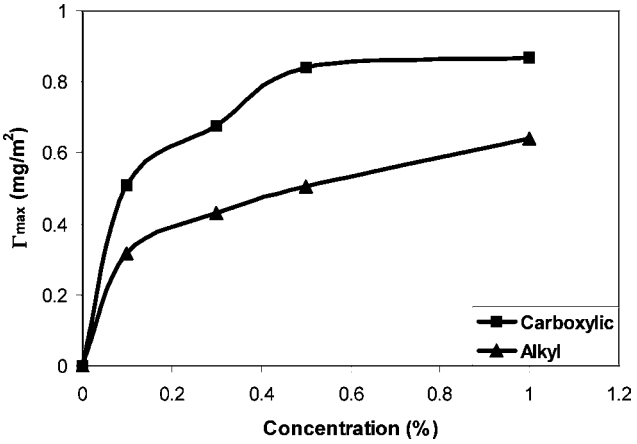

Figure 5. Zein adsorption isotherm on carboxylic and on alkyl SAMs.

authors, however, observed that $[d\Gamma/dt]_0$ on carboxylic surfaces was not linear with concentration and suggested that adsorption rate was surface controlled. Thus zein quality and perhaps bound carotenoids may be a factor influencing adsorption behavior of zein.

Zein adsorption isotherms are shown in **Figure 5**. Maximum zein adsorption, Γ_{max}, increased rapidly with concentration up to 0.1% and then proceeded at a slower rate on both surfaces. The magnitude of the initial slope of the adsorption isotherm is considered an indication of protein affinity for a specific surface (*11*). In **Figure 5**, zein shows higher adsorption on carboxylic surfaces, indicating a higher affinity for carboxylic than for alkyl surfaces, consistent with the observations of Wang and co-workers (*4*) for HCC zein.

Figures 2 and **3** also show desorption curves from zein-saturated surfaces when washed with 75% 2-propanol. Flushing zein-saturated surfaces with 75% 2-propanol would wash off loosely bound or overlaid zein molecules. For the lowest concentration (0.1%) rinsing had no appreciable effect, suggesting the slow-forming zein coating was saturated and uniform. At higher zein concentrations, from 0.3 to 1.0%, $\Gamma_{flushed}$ approached the same value as that of the 0.1% solution, more rapidly for the 1-octanethiol surface than for the 11-mercaptoundecanoic acid. Detection of different $\Gamma_{flushed}$ values on each of the two surfaces indicated the formation of zein layers specific for each surface whose morphology depended on the surface character. The average $\Gamma_{flushed}$ value for carboxylic surfaces was 0.64 and 0.33 mg/m^2 for alkyl surfaces. Wang et al. (*4*) when studying HCC zein adsorption on 1-octanethiol and 11-mercaptoundecanoic acid surfaces also found that both, maximum adsorption and $\Gamma_{flushed}$, were higher on carboxylic than on alkyl

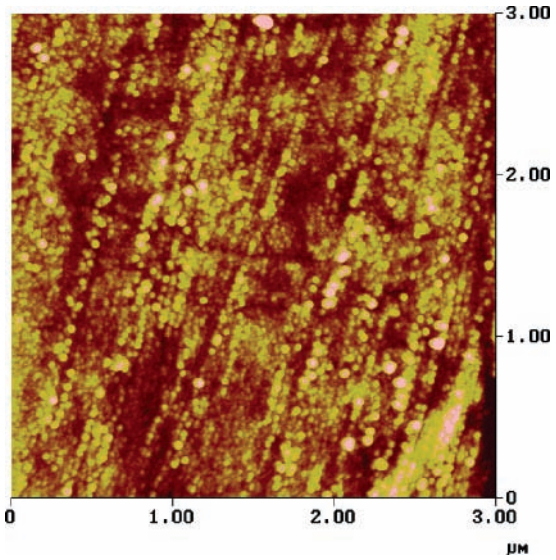

Figure 6. A typical AFM image of gold deposits on SF10 glass slide. The data scale height is 10 nm.

SAMs. They reported $\Gamma_{flushed}$ of 0.55 mg/m^2 for carboxylic surfaces and 0.11 mg/m^2 for alkyl surfaces.

The surface of zein molecules is thought to have sharply defined polar and nonpolar domains. According to the structural model by Matsushima et al. (*12*), zein polar surfaces are located at the top and bottom faces of a prismlike molecule and nonpolar surfaces at the prism sides, corresponding to the α-helix surfaces. The area of each polar face was estimated at 170 Å × 12 Å, while that of nonpolar faces at 170 Å × 46 Å, resulting in a larger zein footprint on hydrophobic surfaces. It is thus expected for zein to interact with both polar and nonpolar groups; however, the mass/area of adsorbed layers on carboxylic or alkyl surfaces may be affected by the different zein footprint on those surfaces.

LCC zein showed higher $\Gamma_{flushed}$ values than HCC zein. On carboxylic surfaces, the difference observed (14%) may be caused by the different experimental setup, including the flow rate of zein solution and SAMs preparation method, and by the higher protein content of the LCC sample. On alkyl surfaces, the difference in $\Gamma_{flushed}$ values was 66%. The larger difference may be related to protein aggregation in the LCC samples.

AFM Results.

A typical topography of gold deposits on SF10 glass slides is shown in **Figure 6**. Its roughness, calculated based on the root-mean-square (RMS) deviation from the average height of peaks above the background, is 1.3 nm. In general, the glass surface was uniformly covered with gold grains. Observed roughness may reflect the roughness of the glass slide underneath. Surfaces of 11-mercaptoundecanoic acid and 1-octanthiol SAMs showed a similar topography as gold surfaces (images not show). This observation was expected since the size of thiol molecules is comparatively small and no aggregation is normally observed.

AFM images were recorded for the surfaces of zein deposits from the SPR experiment (0.3% zein runs). Images were taken from deposits on carboxylic or alkyl surfaces, before and after

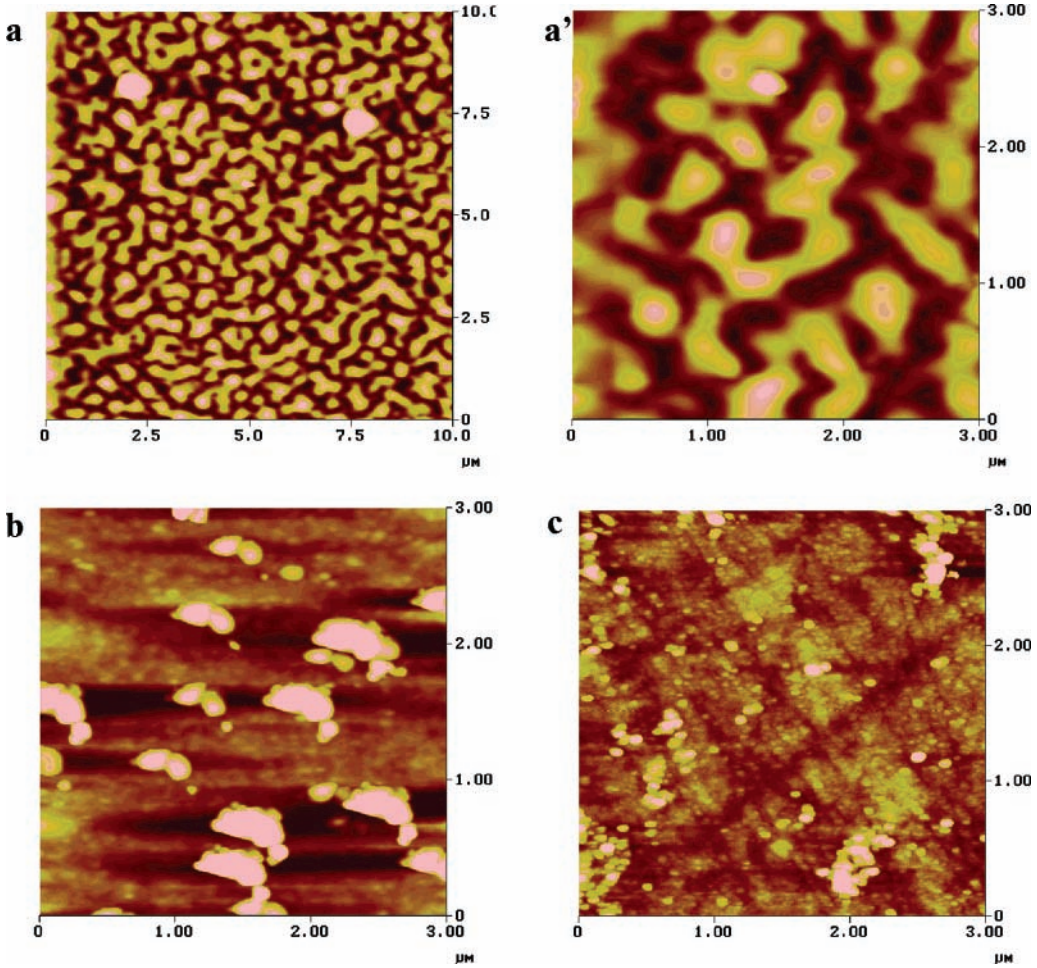

Figure 7. Zein deposition on 11-mercaptoundecanoic acid. (**a** and **a′**) Not washed; (**b**) washed with distilled water; (**c**) washed with 75% 2-propanol. The data scale height for **a**, **a′**, and **b** is 50 nm and for c is 10 nm).

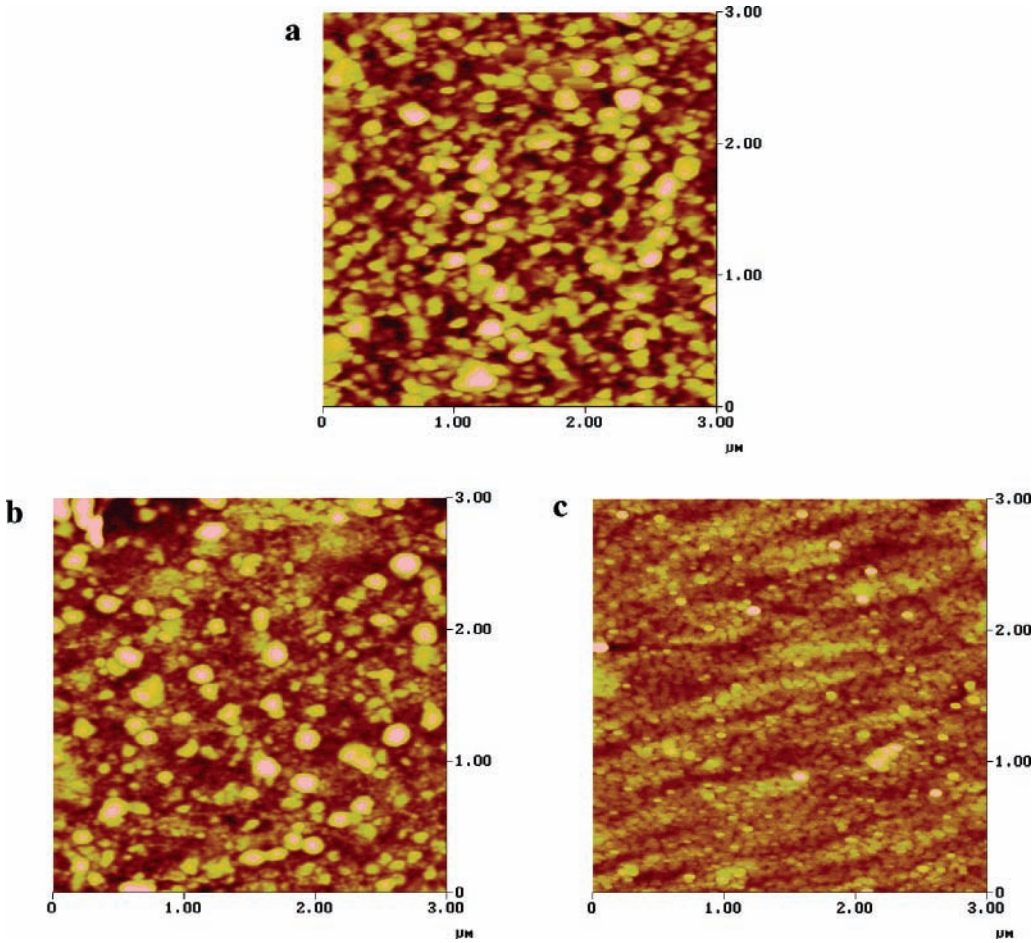

Figure 8. Zein deposition on 1-octanthiol. (**a**) Not washed; (**b**) washed with distilled water; (**c**) washed with 75% 2-propanol. The data scale height for **a** and **b** is 25 nm and for **c** is 10 nm).

flushing with 2-propanol solution or distilled water. SPR slides were dried in a desiccator (RH = 0) at room temperature for 24 h previous to AFM imaging. Typical AFM images are shown in **Figures 7** and **8**. On carboxylic surfaces, before flushing, structures were observed in a range of shapes such as filaments, loops, and toroids, uniformly distributed on the surface (Figure 6a). Guo and co-workers (*13*) reported observing filaments after zein was stretched using molecular combing method. Similar structures were also seen by McMaster et al. (*14*) when ω-gliadin was adsorbed on mica film. The height of AFM features was ~50 nm as determined by section analysis. The calculated roughness was 13.0 nm. When zein-saturated surfaces were flushed with distilled water in the SPR experiment, their topography changed substantially (**Figure 7b**). Filaments and loops disappeared and large aggregates were formed on the surfaces. The image illustrates the aggregation of zein molecules. Two or more ellipsoidal hillocks moved together to form larger structures, of height around 45 nm, roughness 14.5 nm, and grain size 300−500 nm. Interestingly, zein aggregates showed the same orientation, maybe that of the flowing direction or evaporation of water. Aggregation was explained by considering that zein used its polar ends to interact with the carboxylic surface, while exposing its nonpolar sides to the solvent. Therefore, when flushing distilled water over the surface and subsequent drying, the quick change in polarity of the medium prompted zein molecules to join each other through hydrophobic interaction in order to minimize its exposed surface. In an analogous situation, HCC zein formed ring-shaped structures (*3*). However, when the surface was flushed with 2-propanol solution, AFM images (**Figure 7c**) showed that the protein mass accumulated on the surfaces decreased after flushing and subsequent drying, consistent with the SPR measurements reported above. Presumably, loosely bound zein deposits were redissolved in the fresh 2-propanol solution and removed from the surface.

On alkyl surfaces, zein deposits appeared to form uniformly distributed globules, as shown in **Figure 8**. At maximum adsorption, before flushing, the population of globules was high with a maximum height of ~25 nm and calculated roughness of 4.6 nm. Grain size was narrowly distributed between 125 and 150 nm. After washing with distilled water, the globule population went down slightly. Roughness and grain size did not vary appreciably, suggesting the total zein mass remained the same. In this case, there was no evidence of zein aggregation (**Figure 8b**). When the environmental polarity changed from slightly hydrophobic (alcohol−water) to markedly hydrophilic (water), zein used its polar ends, which were available, to interact with water molecules and prevent aggregation. Roughness decreased only to 4.1 nm. When surfaces were flushed with 2-propanol solution, the population of globules decreased appreciably as evidenced by the decreasing roughness (1.03 nm), leaving a layer of zein molecules specific for that surface.

The above experiments illustrated the adsorption and self-assembly properties of zein. Adsorption kinetics and surface morphology were influenced by surface and media polarity. LCC zein showed differences in adsorption behavior with respect to HCC zein, as reported by Wang et al. (*3*, *4*), which may be attributable to its lower lipid content. Further research is needed to clarify the effect of bound materials on adsorption properties of zein.

ACKNOWLEDGMENT

We would like to thank Dr. Paul Bohn for allowing the use of SPR equipment.

LITERATURE CITED

(1) Lai, H.-M.; Padua, G. W. Properties and microstructure of plasticized zein films. *Cereal Chem.* **1997**, *74*, 771−775.
(2) Wang, Q. Investigation of protein-fatty acid interactions in zein films. Ph.D. dissertation, 2004, University of Illinois at Urbana−Champaign.
(3) Wang, Q.; Crofts, A. R.; Padua, G. W. Protein−lipid interactions in zein films investigated by surface plasmon resonance. *J. Agric. Food Chem.* **2003**, *51*, 7439−7444.
(4) Wang, Q.; Wang, J.-F.; Geil, P. H.; Padua, G. W. Zein adsorption to hydrophilic and hydrophobic surfaces investigated by surface plasmon resonance. *Biomacromolecules* **2004**, *5*, 1356−1361.
(5) Cimitan, S.; Lindgren, M. T.; Bertucci, C.; Danielson, U. H. Early absorption and distribution analysis of antitumor and anti-AIDS drugs: Lipid membrane and plasma protein interactions. *J. Med. Chem.* **2005**, *48*, 3536−3546.
(6) Dahlin, A.; Zach, M.; Rindzevicius, T.; Kall, M.; Sutherland, D. S.; Hook, F. Localized surface plasmon resonance sensing of lipid-membrane-mediated biorecognition events. *J. Am. Chem. Soc.* **2005**, *127*, 5043−5048.
(7) Zeng, Z. X.; Zhao, Y.; Hao, Y. H.; Tan Z. Tetraplex formation of surface-immobilized human telomere sequence probed by surface plasmon resonance using single-stranded DNA binding protein. *J. Mol. Recognit.* **2005**, *18*, 267−271.
(8) Esen, A. A proposed nomenclature for alcohol-soluble proteins (zeins) of maize (Zea mays L.). *J. Cereal Sci.* **1987**, *5*, 117−128.
(9) Wang, J.-F.; Geil, P. H.; Kolling, R. J.; Padua, G. W. Analysis of zein by matrix-assisted laser desorption/ionization mass spectrometry. *J. Agric. Food Chem.* **2003**, *51*, 5849−5854.
(10) Dickey, L. C.; Parris, N.; Craig, J. C.; Kurantz, M. J. Ethanolic extraction of zein from maize. *Ind. Crops Prod.* **2001**, *13*, 67−76.
(11) Haynes, C. A.; Norde, W. Globular proteins at solid/liquid interfaces. *Colloids Surf., B* **1994**, *2*, 517−566.
(12) Matsushima, N.; Danno, G. I.; Takezawa, H.; Izumi, Y. Three-dimensional structure of maize α-zein proteins studied by small-angle X-ray scattering. *Biochim. Biophys. Acta* **1997**, *1339*, 14−22.
(13) Guo, Y.; Liu, Z.; An, H.; Li, M.; Hu, J. Nano-structure and properties of maize zein studied by atomic force microscopy. *J. Cereal Sci.* **2005**, *41*, 277−281.
(14) McMaster, T. J.; Miles, M. J.; Wannerberger, L.; Eliasson, A.-C.; Shewry, P. R.; Tatham, A. S. Identification of microphases in mixed α- and ω-gliadin protein films investigated by atomic force microscopy. *J. Agric. Food Chem.* **1999**, *47*, 5093−5099.

Received for review June 28, 2005. Revised manuscript received October 26, 2005. Accepted November 4, 2005. This work was supported in part by the Illinois Corn Marketing Board. We appreciate the help from the Center for Microanalysis of Materials, University of Illinois, which is partially supported by the U.S. Department of Energy under Grant DEFG02-91-ER45439.

JF051545L